A PARAMETRIC MODELING APPROACH FOR WIRELESS CAPSULE ENDOSCOPY HAZY IMAGE RESTORATION

*Y. Wang[1], C. Cai[2], J. Liu[1], Y. X. Zou[1]**

[1]ADSPLAB/ELIP, School of ECE, Peking University, Shenzhen 518055, China
[2]Department of Computer Science, College of Information Engineering, Northwest A&F University, Yangling 712100, China

ABSTRACT

Wireless capsule endoscopy (WCE) is an innovative solution for gastrointestinal disease detection. The image quality of WCE is not satisfactory for medical applications since some of them are dark or hazy. For the purpose of improving WCE image quality, we take a new way to establish a parametric image generation model (called WCE hazy model) between the captured image and the ideal image by considering adverse effects due to inhomogeneous lighting, unfocused and light reflection. Some experiments have been carried out to validate this model. Accordingly, the retinex theory and dark-channel prior have been adopted to estimate the model parameters adaptively. Hence, the WCE hazy image restoration is achieved by the inverse process of the hazy model. Intensive experiments have been conducted with hazy WCE images of the testers. Experimental results using the subjective and objective performance measures further verify the effectiveness of proposed method.

Index Terms—wireless capsule endoscopy, image restoration, parametric generation model, retinex theory, dark-channel prior

1. INTRODUCTION

In the past year, digestive system cancer had been the second cancer-related killer in U.S.A. and caused 61,950 death [1]. Early detection and treatment of gastrointestinal disease are very crucial. Wireless capsule endoscopy (WCE) is an innovative solution for gastrointestinal disease detection. It was invented in 2000 and put in use in 2001 [2]. However, the images captured by WCE system are not as good as those taken by traditional endoscopy due to several hardware constraints [3]: 1) the battery capacity is limited resulting in inhomogeneous lighting, 2) the camera used in WCE is low-focal-length camera which may produce unfocused images; 3) complicated circumstance of gastrointestinal tract and moving imaging method also lead to poor image quality. Fig. 1 shows several WCE images with low quality, where Figs. 1 (1) and (2) are with weak lighting, Figs. 1 (3) and (4) are hazy, which provide less diagnostic information for physicians. As a result, the image quality improvement is highly demanded in WCE medical applications. There are several image enhancement approaches, such as histogram equalization-related methods [4], Filter based methods [5], transform domain based methods [6], and anisotropic diffusion based approaches [3, 7]. Experimental results show that these methods have some good effects on enhancing low-luminosity or low-contrast images, but don't have desired effect in handling hazy images. Moreover, it is noted that the hazy images do not lack luminosity while they have distorted color and low-contrast properties. Viewed from another perspective, the hazy effect is similar to the blurred effect which usually is caused by motion or poor focusing. The blurred image could be restored under the convolution model by using the inverse filtering in its frequency domain. Wiener filtering is widely used and quite effective in solving deblurring problem [8, 9], but it needs pre-set parameters chosen by trial and error, which is impractical without the knowledge of point spread function (PSF). Besides, whether the hazy effect of WCE images equals to blurred effect is unknown. Some discussions are presented in Section 2. In this circumstance, a more general model is expected to handle the quality improvement of the hazy images.

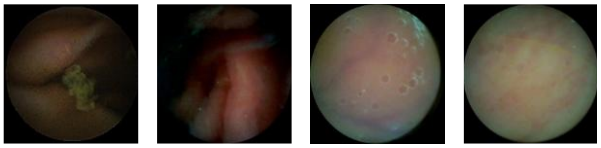

(1) (2) (3) (4)

Fig. 1. Low quality WCE images (Dark and hazy)

By investigating the mechanism of the WCE image generation process, we believe that inhomogeneous distributed illumination and lost focusing are main factors contributing to the low quality of WCE images. Motivated by the methods developed for removing the fog from the natural images, in this paper, we make an effort to establish the parametric image generation model (called hazy model here) between the captured image and the ideal image by considering adverse effects due to the inhomogeneous lighting, unfocused and light reflection. To make the problem tractable, the following assumptions are made: 1) the captured WCE image has a counterpart ideal image. 2) the transformation of the ideal image to the capture image is nonlinear but can be modeled in a parametric way. 3) the parameters can be estimated.

In the rest of this paper, Sec. 2 introduces a parametric WCE image generation model and the validation of the model by experiments. Sec. 3 shows the derivation of the adaptive WCE image restoration algorithm. Sec. 4 presents the experimental results and performance analysis. Finally, Sec. 5 gives the conclusion.

2. PROBLEM FORMULATION

In natural image dehazing research, the most commonly used imaging model for images is the additive model given as [10, 11]:

$$I(x,y) = T(x,y)R(x,y) + [1 - T(x,y)]a \quad (1)$$

where (x,y) is the pixel index. $\boldsymbol{I}$ and $\boldsymbol{R}$ are the generated or observed image and ideal image (scene radiance), respectively. $\boldsymbol{T}$ is the transmission matrix and $T(x, y) \in (0,1)$. Transmission is the property of a substance to permit the passage of light. Here the element of $\boldsymbol{T}$ is a ratio of scene radiance reaching the camera. a is the global atmospheric light. It is constant due to its homogeneousness.

In this study, we follow the same spirit in (1) to model WCE images. Obviously, for generating WCE images, the ambient illumination was created by multi light sources, so it is no longer homogeneous and shows the inhomogeneous property. Thus it is reasonable to establish a generation model for WCE images as follows:

$$I(x,y) = T(x,y)R(x,y) + [1 - T(x,y)]L(x,y) \quad (2)$$

where $\boldsymbol{L}$ is the inhomogeneous ambient illumination presented in imaging procedure. From (2), $\boldsymbol{I}$ can be seen as the composition of weighted scene radiance $\boldsymbol{R}$ and weighted ambient illumination $\boldsymbol{L}$. It is clear that the weights are controlled by the transmission $\boldsymbol{T}$. Carefully examining (2), we have the following observations:

1） When $T(x, y) = 0$, (2) gives $I(x, y) = L(x, y)$. This indicates that no information of scene radiance left in $\boldsymbol{I}$, so it's impossible to recover $\boldsymbol{R}$ from $\boldsymbol{I}$.

2） When $T(x, y) \in (0,1)$ but $L(x, y) = 0$, (2) turns to be the multiplicative model denoted as [12]

$$I(x,y) = T(x,y)R(x,y) \quad (3)$$

where $\boldsymbol{I}$ is a portion of $\boldsymbol{R}$ and can be roughly estimated by image enhancement algorithms such as histogram equalization.

3） When $T(x, y) \in (0,1)$ while $L(x, y) > 0$, (2) presents its general form and $\boldsymbol{I}$ is influenced by $\boldsymbol{R}$, $\boldsymbol{L}$ and their responding weight.

4） When $T(x, y) = 1$, (2) shows the ideal imaging status and we have $I(x, y) = R(x, y)$. Unluckily, this case rarely occurs in real applications.

In order to put model (2) in use, we propose the following in modelling approaches for transmission $\boldsymbol{T}$ and illumination $\boldsymbol{L}$. Following the research in [13], transmission $\boldsymbol{T}$ for WCE imaging can be modeled as

$$I_{temp}(x,y) = \sum_{n=1}^{N} \omega_n F_n(x,y) * R(x,y) \quad (4)$$

$$T(x,y) = \frac{I^g_{temp}(x,y) - \min(\boldsymbol{I}^g_{temp})}{\max(\boldsymbol{I}^g_{temp}) - \min(\boldsymbol{I}^g_{temp})} \quad (5)$$

where ω_n is the weight, $\sum_{n=1}^{N} \omega_n = 1$ and in our study $\omega_n = 1 / N$, $N = 3$. $F_n(x, y)$ is a multi-scale Gaussian function with the standard deviation σ_n, where σ_n is set to different values at each n. * is the convolution operator. It can be seen that model (4) simulates the transmission property by applying the multi-scale Gaussian blurring effects on $\boldsymbol{R}$. In addition, (5) gives the normalized transmission model where we assume the transmission $T(x, y)$ is proportional to $I^g_{temp}(x, y)$. $\boldsymbol{I}^g_{temp}$ is the grayscale version converted from $\boldsymbol{I}_{temp}$ from RGB channels.

Now, let's consider illumination $\boldsymbol{L}$ for WCE imaging. Motivated by the research in [14], it will be a good option to model $\boldsymbol{L}$ as:

$$L(x,y) = F(x,y) * R(x,y) \quad (6)$$

where $F(x, y)$ is a single Gaussian function, which is able to model inhomogeneous global illumination properly.

So far, we have established the general WCE image generation model by (2), (5) and (6). Let's have a demonstration. We select

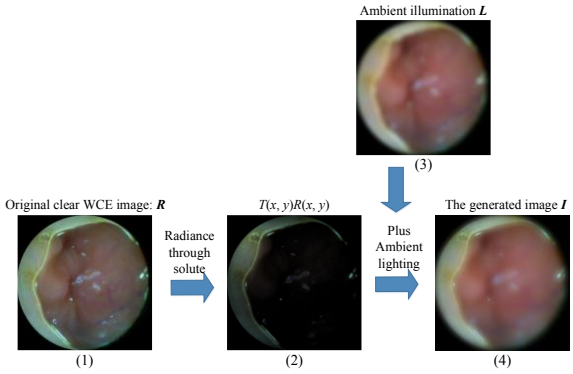

Fig. 2. WCE hazy image generation

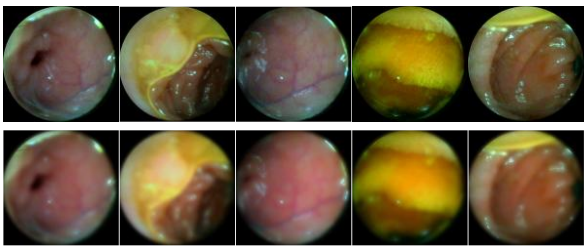

Fig. 3. Synthetic hazy effect. First row shows clear images and second rows shows generated hazy images.

one good quality WCE image as $\boldsymbol{R}$ shown in Fig. 2 (1). If illumination $\boldsymbol{L}$ is zero or close to zero, but the transmission is modeled in (5), the resulting image by model (2) is shown in Fig. 2 (2). We can see that the quality of the image $\boldsymbol{R}$ has been degraded greatly due to the transmission matrix $\boldsymbol{T}$. Moreover, comparing the image in Fig. 2 (2) with the images in Figs. 1 (1) and (2), it is easy to observe their similarities with dark and low contrast properties. This may explain the dark WCE images are generated due to low transmission. Fig. 2 (3) is generated by (6). It is a typical blurred image where global illumination is improved and some informative details are smoothed. Just like bubble locates in top left corner which can be observed in Figs 2 (1) and (4), it vanishes in Fig. 2 (3) where it is expected to be shown.

Moreover, If transmission and illumination are all non-ideal, which are modeled in (5) and (6), the WCE image $\boldsymbol{I}$ generated by model (2) is shown in Fig. 2 (4). It is easy to identify that image in Fig. 2 (4) presents some common features of the hazy images shown in Figs. 1 (3) and (4). They all look low contrast and global bright, and still contain some informative details.

By the comparisons between Fig. 2(3) and Fig. 2(4), and between Fig. 2 (4) and Figs 1 (3) (4), it is easy to identify the differences between the blurred image and the hazy image. The latter contains more useful information about $\boldsymbol{R}$ than the former. With the discussion shown above, it is not appropriate to use traditional convolution model designed for blurred images to deal with WCE hazy problem.

More synthesized hazy WCE images by the proposed model in (2) are shown in Fig. 3. Comparing the synthesized hazy images in Fig. 2 and Fig. 3 with those in Fig. 1, we may conclude that the proposed generation model (2) is suitable for modeling the real WCE hazy images. As a result, if illumination $\boldsymbol{L}$ and transmission matrix $\boldsymbol{T}$ can be estimated properly, it is straightforward to recover $\boldsymbol{R}$ from $\boldsymbol{I}$ by solving the inverse problem of model (2) and the recovered $\boldsymbol{R}$ will have improved quality compared with $\boldsymbol{I}$.

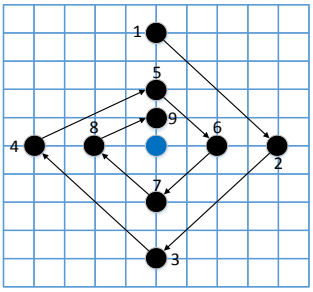

Fig. 4. The sequence of translation vectors for the D_n in FMR

3. THE PROPOSED WCE HAZY IMAGE RESTORATION METHOD

In this section, we will first present the estimation methods for $\boldsymbol{T}$ and $\boldsymbol{L}$, respectively. Then the proposed parametric modeling based WCE hazy image restoration (WCE-PM-HIR) method will be introduced in details.

3.1. The estimation of ambient illumination

As assumed in Section 2, illumination $\boldsymbol{L}$ is normal distributed modeled in (6). Here, we need to estimate $\boldsymbol{L}$ from the captured WCE image $\boldsymbol{I}$. In our study, Frankle-McCann Retinex (FMR) approach is adopted to solve this problem. In FMR theory, it assumes that the illumination in pixel (x, y) is not only affected by its neighboring pixels, but also by the pixels at far distance, which makes image illumination looks more natural. According to [15, 16], the estimation of illumination $\boldsymbol{L}$ using FMR method can be implemented as follows: the illumination $\boldsymbol{L}_0$-hat is initialized to be the maximum value of observed image $\boldsymbol{I}$, then FMR executes the iterative procedure:

$$\hat{\boldsymbol{L}}_{n+1} = \max\{\frac{\hat{\boldsymbol{L}}_n + \boldsymbol{I}}{2}, \frac{\hat{\boldsymbol{L}}_n + D_n(\hat{\boldsymbol{L}}_n)}{2}\} \tag{7}$$

where $\boldsymbol{L}_n$-hat is the estimated illumination by iterative approach, which will be assigned to $\boldsymbol{L}$ when iteration is stopped. $D_n(.)$ is a spatially shifting operator which will shift the image by the n^{th} element of a sequence of spirally decaying translation vectors $\{\boldsymbol{d}_n\}$, where $\boldsymbol{d}_n$ can be denoted as $\boldsymbol{v}_{n,n+1}$, just as shown in Fig. 4. The relation between two adjacent translation vectors satisfy: $|\boldsymbol{d}_n| = 2|\boldsymbol{d}_{n+1}|$. The iteration of FMR will be terminated when $|\boldsymbol{d}_n| <= 1$. Specific details can be referred to [16].

3.2. Estimation of Transmission

After we get the estimation of $\boldsymbol{L}$, we need to estimate the transmission $\boldsymbol{T}$ from $\boldsymbol{I}$ based on model (2). Motivated by the research in [11], we solve this problem based on the dark-channel prior (DCP).

To make the presentation completeness, the dark-channel prior is briefly introduced first. It is noted that DCP is concluded from analyzing the statistics of outdoor haze-free images [11]. It finds that in most non-sky regions, at least one color channel has some pixels whose intensity is very low (close to zero, called dark channel), which can be formulated as:

$$R^{dark}(x,y) = \min_{(\bar{x},\bar{y})\in\Omega(x,y)} \left\{ \min_{c\in\{\text{r,g,b}\}} \left(R^c(\bar{x},\bar{y}) \right) \right\} \to 0 \tag{8}$$

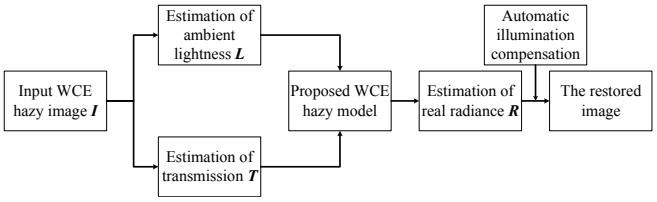

Fig. 5. The diagram of the WCE hazy image restoration algorithm (WCE-HIR)

where $\boldsymbol{R}^c$ indicates the c channel image of $\boldsymbol{R}$, $\Omega(x, y)$ is an image patch which centers at (x, y), and $(\bar{x}, \bar{y})$ is a pixel index in patch Ω.

For $\boldsymbol{R}^c$, from (2), by normalizing related illumination, it yields:

$$\frac{I^c(x,y)}{L^c(x,y)} = \frac{R^c(x,y)}{L^c(x,y)} T(x,y) + 1 - T(x,y) \tag{9}$$

As noted in Section 2, the transmission $\boldsymbol{T}^c$ is modeled by (4) and (5), so it is reasonable to assume $\boldsymbol{T}^c$ as a constant over the patch $\Omega(x, y)$, which is denoted as $T_p(x,y)$, and then putting the minimum operator on both sides of (9) gives:

$$\min_{(\bar{x},\bar{y})\in\Omega(x,y)} \{ \min_{c\in\{\text{r,g,b}\}} (I^c(\bar{x},\bar{y}) / L^c(\bar{x},\bar{y})) \} = m + 1 - T_p(x,y) \tag{10}$$

where $m = \min_{(\bar{x},\bar{y})\in\Omega(x,y)} \{ \min_{c\in\{\text{r,g,b}\}} (R^c(\bar{x},\bar{y}) / L^c(\bar{x},\bar{y})) \} T_p(x,y)$.

If the condition in (8) satisfied, then m is zero or close to zero. Then with simple manipulations, from (10), we can derive:

$$T_p(x,y) = 1 - \min_{(\bar{x},\bar{y})\in\Omega(x,y)} \{ \min_{c\in\{\text{r,g,b}\}} (I^c(\bar{x},\bar{y}) / L^c(\bar{x},\bar{y})) \} \tag{11}$$

In practice, if all the hazy effect is removed, we may lose the feeling of depth and feel unnatural. So a constant parameter λ is introduced into equation (11) to preserve a small amount of haze. Then we get:

$$T_p(x,y) = 1 - \lambda \min_{(\bar{x},\bar{y})\in\Omega(x,y)} \{ \min_{c\in\{\text{r,g,b}\}} (I^c(\bar{x},\bar{y}) / L^c(\bar{x},\bar{y})) \} \tag{12}$$

Based on experiments, we find λ=0.75 is the best for WCE visualization.

3.3 The Recovery of Scene Radiance

With the estimated values of ambient illumination and transmission matrix described in Sec. 3.1 and 3.2, the scene radiance $R(x, y)$ can be estimated directly using model (2). Moreover, it is practical to restrict the transmission by a lower bound t_0 to avoid it close to zero in case $R(x, y)$ is irrecoverable. Therefore, we reach the following:

$$\tilde{R}(x,y) = \frac{I(x,y) - L(x,y)}{max(T_p(x,y), t_0)} + L(x,y) \tag{13}$$

where t_0 is set to be 0.05 in our study.

In our research, we noted that the scene radiance computed by the WCE-PM-HIR method may look darker in some case, because of the removal of ambient illumination. To deal with this situation, the illumination compensation approach is developed as follows. Through several comparisons between the global illumination of the estimated scene radiance and that of corresponding original image, we propose to compensate scene radiance as follows:

$$\tilde{\boldsymbol{R}} = \begin{cases} \tilde{\boldsymbol{R}}, \text{if } |g(\tilde{\boldsymbol{R}} - \boldsymbol{I})| < \Delta l \\ comp(\tilde{\boldsymbol{R}}), \text{else} \end{cases} \tag{14}$$

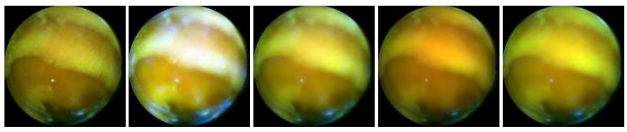

(1) Original (2) FMR (3) AAD (4) HR-DCP (5) WCE-PM-HIR

Fig. 6. Clear image and its restored images

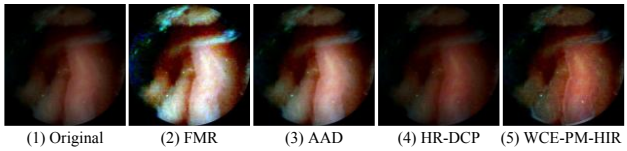

(1) Original (2) FMR (3) AAD (4) HR-DCP (5) WCE-PM-HIR

Fig. 7. Dark image and its restored images

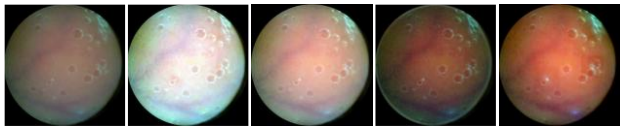

(1) Original (2) FMR (3) AAD (4) HR-DCP (5) WCE-PM-HIR

Fig. 8. Hazy image and its restored images

where $g(.)$ is a function to measure the difference between the estimated scene radiance and the captured image $\boldsymbol{I}$, Δl is a threshold value, *comp*(.) is a method or procedure to improve illumination of the image. In this study, we select the adaptive anisotropic diffusion method as the compensation approach since it is good at improving illumination and preserving details. The proposed WCE-PM-HIR algorithm described in this section is summarized in Fig. 5.

4. EXPERIMENTS AND RESULTS

In this section, several experiments have been carried out based on WCE images supplied from Shenzhen JiFu Technology Ltd., which were captured data from trial patients. The size of WCE images is 480×480 with RGB three channels. We compared the results of our proposed method with that of three existing methods including the FMR [16], adaptive anisotropic diffusion (AAD) [3, 7] and haze removal based on dark-channel prior (HR-DCP) [11]. First of all, to obtain objective performance of our proposed WCE-PM-HIR, 15 clear WCE images are picked as known ideal images, then the proposed WCE parametric image generation model in (2) is used to generate low quality images, which then will be restored by different algorithms mentioned above. The peak signal-to-noise ratio (PSNR) and the averaged structural similarity (SSIM) [17] are used to measure the performance of the algorithms. The results are shown in Table 1. One visual example is shown in Fig. 6.

In Table 1, it is clear to see that proposed WCE-PM-HIR outperforms other algorithms from objective evaluation. It gets the highest value in PSNR and SSIM in most cases out of 15 or on average. Specifically, the PSNR value of WCE-PM-HIR is higher about 2.84dB than that of HR-DCP and higher about 7.93dB than that of AAD on average. The SSIM index of WCE-PM-HIR is higher about 1.50% that that of HR-DCP and higher about 1.14% than that of AAD on average. It is conclude that WCE-PM-HIR does recover much more useful information (color and local details) of $\boldsymbol{R}$ from $\boldsymbol{I}$ than other algorithms.

In synthetic case Fig. 6, it is clear to see that FMR performs worst. Although the resulting global illumination is brightest, it fails to recover the true color of the original image. The illumination of the image produced by AAD is a little darker, but it performs well in recovering local details. HR-DCP and our proposed WCE-PM-HIR all performed well to recover color and some local details. They look quite similar in visualization, but the WCE-PM-HIR performs better in color restoration.

Table 1 PSNR and SSIM results

No.	PSNR(dB)				SSIM(%)			
	FMR	AAD	HR-DCP	WCE-PM-HIR	FMR	AAD	HR-DCP	WCE-PM-HIR
1	15.19	19.91	25.82	**26.90**	89.45	94.16	93.37	**94.95**
2	15.57	20.52	27.19	**30.51**	88.38	93.60	94.42	**95.10**
3	16.40	22.15	26.53	**28.81**	89.81	94.58	94.61	**95.32**
4	14.13	25.22	23.99	**29.39**	84.80	**95.54**	93.11	95.33
5	11.29	21.41	24.64	**30.87**	77.22	93.82	92.66	**94.68**
6	12.99	16.60	22.57	**24.56**	83.36	90.21	**94.68**	94.39
7	11.21	20.84	21.78	**29.23**	78.96	94.43	91.46	**95.57**
8	12.91	22.77	20.93	**24.58**	83.66	**95.15**	91.2	93.78
9	12.37	19.72	21.43	**29.47**	82.52	93.21	90.29	**94.65**
10	11.65	23.92	20.44	**25.07**	79.08	**95.32**	88.01	93.11
11	15.47	20.61	**34.17**	33.70	85.03	94.53	**97.24**	97.12
12	15.05	22.01	34.70	**35.20**	87.91	95.87	97.42	**97.49**
13	14.73	19.64	31.66	**33.75**	88.20	94.38	96.66	**97.33**
14	17.58	23.02	30.71	**32.06**	90.80	95.24	96.24	**96.27**
15	14.26	16.76	**24.83**	19.93	90.03	93.38	**96.59**	95.28
avg	14.05	21.01	26.09	**28.94**	85.28	94.22	93.86	**95.36**

Moreover, the experimental results for improving the low quality WCE images are shown in Fig. 7 and Fig. 8. From Fig. 7, where the original image is a low illumination one, it can see that WCE-PM-HIR is inferior to AAD but superior to FMR and HR-DCP. However, from Fig. 8, where the original image is a hazy image, we can see WCE-PM-HIR outperforms other algorithms for visualization purpose. Especially, HR-DCP and WCE-PM-HIR work well in recovering color information and improving the contrast for hazy images. However, from the results in Table 1, we can see that HR-DCP recovers more unwanted information (noise) than WCE-PM-HIR. From all results shown above, it is quite confident that our proposed WCE-PM-HIR algorithm is quite effective both in visual perception and quality improvement for hazy WCE images.

5. CONCLUSION

This paper works on WCE hazy image restoration problem. Motivated by the general image generation model, a hazy WCE image generation model is proposed based on certain assumptions. The retinex and dark-channel prior theory have been employed to estimate the model parameters. Intensive experimental results verify the effectiveness of the proposed WCE hazy image restoration method. Results show that the proposed WCE-PM-HIR method is able to improve the contrast, color and local details of the degraded WCE images, which makes the recovered images look more visual attractive.

ACKNOWLEDGMENT

This work was partially supported by the Shenzhen Science & Technology Fundamental Research Program (No: JCYJ20130329175141512).

REFERENCE

[1] R. Siegel, D. Naishadham, and A. Jemal, "Cancer statistics, 2013," *CA: A Cancer Journal for Clinicians,* vol. 63, pp. 11-30, 2013.

[2] G. Iddan, G. Meron, A. Glukhovsky, and P. Swain, "Wireless capsule endoscopy," *Nature,* vol. 405, p. 417, 2000.

[3] L. Li, Y. Zou, and Y. Li, "Wireless capsule endoscopy images enhancement based on adaptive anisotropic diffusion," in *Signal and Information Processing (ChinaSIP), 2013 IEEE China Summit & International Conference on*, pp. 273-277, 2013.

[4] M. Abdullah-Al-Wadud, M. H. Kabir, M. A. A. Dewan, and O. Chae, "A dynamic histogram equalization for image contrast enhancement," *Consumer Electronics, IEEE Transactions on,* vol. 53, pp. 593-600, 2007.

[5] A. Polesel, G. Ramponi, and V. J. Mathews, "Image enhancement via adaptive unsharp masking," *Image Processing, IEEE Transactions on,* vol. 9, pp. 505-510, 2000.

[6] J.-L. Starck, F. Murtagh, E. J. Candes, and D. L. Donoho, "Gray and color image contrast enhancement by the curvelet transform," *Image Processing, IEEE Transactions on,* vol. 12, pp. 706-717, 2003.

[7] B. Li and M. Q.-H. Meng, "Wireless capsule endoscopy images enhancement via adaptive contrast diffusion," *Journal of Visual Communication and Image Representation,* vol. 23, pp. 222-228, 2012.

[8] J. Amudha, N. Pradeepa, and R. Sudhakar, "A Survey on Digital Image Restoration," in *International Conference on Modelling Optimization and Computing*. vol. 38, R. Rajesh, K. Ganesh, and S. C. L. Koh, Eds., ed Amsterdam: Elsevier Science Bv, pp. 2378-2382, 2012.

[9] C. Solomon and T. Breckon, *Fundamentals of digital image processing: A practical approach with examples in Matlab*: John Wiley & Sons, 2011.

[10] R. Fattal, "Single image dehazing," *Acm Transactions on Graphics,* vol. 27, Aug 2008.

[11] K. He, J. Sun, and X. Tang, "Single image haze removal using dark channel prior," *Pattern Analysis and Machine Intelligence, IEEE Transactions on,* vol. 33, pp. 2341-2353, 2011.

[12] L. Lei, Y. Zhou, and J. Li, "An Investigation of Retinex algorithms for image enhancement," *Journal of Electronics (China),* vol. 24, pp. 696-700, 2007.

[13] Z.-U. Rahman, D. J. Jobson, and G. A. Woodell, "Multi-scale retinex for color image enhancement," in *Image Processing, 1996. Proceedings., International Conference on*, pp. 1003-1006, 1996.

[14] D. J. Jobson, Z.-U. Rahman, and G. A. Woodell, "Properties and performance of a center/surround retinex," *Image Processing, IEEE Transactions on,* vol. 6, pp. 451-462, 1997.

[15] R. Kimmel, M. Elad, D. Shaked, R. Keshet, and I. Sobel, "A variational framework for retinex," *International Journal of computer vision,* vol. 52, pp. 7-23, 2003.

[16] D.-G. Hwang, W.-R. Lee, Y.-J. Oh, and B.-M. Jun, "Frankle-McCann Retinex by Shuffling," in *Convergence and Hybrid Information Technology*, ed: Springer, pp. 381-388, 2012.

[17] W. Zhou, A. C. Bovik, H. R. Sheikh, and E. P. Simoncelli, "Image quality assessment: from error visibility to structural similarity," *Image Processing, IEEE Transactions on,* vol. 13, pp. 600-612, 2004.